Journal of Organometallic Chemistry, 326 (1987) 99-116
Elsevier Sequoia S.A., Lausanne - Printed in The Netherlands

^1H, ^{13}C and ^{31}P STUDIES OF CYCLOPENTADIENYLRUTHENIUM COMPLEXES WITH CYCLOOCTATETRAENE OR CYCLOOCTADIENE LIGANDS. X-RAY STRUCTURE OF $[(\eta^5\text{-}C_5H_5)Ru(\eta^4\text{-}C_8H_8)(P(OCH_3)_3)]PF_6$

AMY M. McNAIR, THOMAS P. GILL and KENT R. MANN*
Department of Chemistry, University of Minnesota, Minneapolis, MN 55455 (U.S.A.)

(Received May 5th, 1986)

Summary

The X-ray crystal structure of $[(\eta^5\text{-}C_5H_5)Ru(\eta^4\text{-}COT)(P(OCH_3)_3)]PF_6$ (COT = cyclooctatetraene) (formula, $C_{16}H_{22}F_6O_3P_2Ru$) was determined. The compound crystallizes in the monoclinic space group no. 4 $P2_1$ (*a* 11.007(3), *b* 11.066(3), *c* 8.660(3) Å, β 105.56(20)°, $Z = 2$). The structure consists of discrete disordered PF_6^- anions and $[(\eta^5\text{-}C_5H_5)Ru(\eta^4\text{-}COT)(P(OCH_3)_3)]^+$ cations. The cation exhibits a planar, $C_5H_5^-$ unit. (Ru-C distances of 2.221(7) Å), a $P(OCH_3)_3$ ligand (Ru-P distance of 2.306(2) Å) and an η^4-COT ligand in the tub conformation. The η^4-COT ligand is bound to the Ru atom through two different Ru-C bond distances 2.298(5) and 2.223(6) Å, the longer distance appropriate to the Ru-C bonds nearest the Ru-P bond. The ^1H, ^{13}C and ^{31}P NMR spectra of $[(\eta^5\text{-}C_5H_5)Ru(\eta^4\text{-}COT)(P(OCH_3)_3)]PF_6$, $[(\eta^5\text{-}C_5H_5)Ru(\eta^4\text{-}COT)(CO)PF_6$, $[(\eta^5\text{-}C_5H_5)Ru(\eta^6\text{-}COT)PF_6$ and $[(\eta^5\text{-}C_5H_5)Ru(\eta^4\text{-}COD)(P(OCH_3)_3]PF_6$ (COD = 1,5-cyclooctadiene) were obtained. Comparison of the ^1H NMR and ^{13}C spectra of $[(\eta^5\text{-}C_5H_5)Ru(\eta^4\text{-}COT)(P(OCH_3)_3)]PF_6$ and $[(\eta^5\text{-}C_5H_5)Ru(\eta^4\text{-}COD)(P(OCH_3)_3)]PF_6$ confirm that the COT complex retains the solid state structure in solution. Through comparison and simulation of the ^1H and $^1H\{^{31}P\}$ NMR spectra of $[(\eta^5\text{-}C_5H_5)Ru(\eta^4\text{-}COT)(P(OCH_3)_3)]PF_6$ all eight COT protons are found to exhibit $^1H-^{31}P$ coupling. The allylic coupling constants that involve hydrogens bound to a coordinated carbon have small positive values, rather than the small negative values usually found in 'pure' organic systems.

Introduction

While studying the reaction chemistry of $[(\eta^5\text{-}C_5H_5)Ru(CH_3CN)_3]PF_6$ [1], we designed a synthesis for $[(\eta^5\text{-}C_5H_5)Ru(\eta^4\text{-}COT)(P(OCH_3)_3]PF_6$ (COT = cyclooctatetraene) [2]. As a matter of course, we determined the X-ray crystal structure of this compound [2]. In the crystal structure of $[(\eta^5\text{-}C_5H_5)Ru(\eta^4\text{-}$

0022-328X/87/$03.50

$C_8H_8)(P(OCH_3)_3)]PF_6$, the cyclopentadienyl ligand is bound in the traditional η^5 manner, the trimethylphosphite phosphorus is bound directly to the ruthenium metal center and the cyclooctatetraene ligand is bound η^4 through carbons one, six, two and five, in the familiar tub conformation. However, the 80 MHz ^1H NMR solution spectrum seemed to be inconsistent with this formulation. An unexpected downfield shift of approximately 0.2 ppm was observed in the methyl phosphite resonances relative to other known Ru^{II} compounds containing both cyclopentadienyl and phosphite ligands [1]. Additionally, the $^1H-^{31}P$ coupling routinely observed between the cyclopentadienyl protons and the coordinated phosphite phosphorus atom was absent. Finally, additional large couplings only attributable to $^{31}P-^1H$ coupling were observed in the COT resonances [2]. These results led us to speculate that the solution structure of $[(\eta^5-C_5H_5)Ru(\eta^4-COT)(P(OCH_3)_3)]PF_6$ might be significantly different from the one adopted in the crystalline state. An intriguing possibility that we entertained to explain our data involved the rearrangement of the solid state structure on dissolution to one that contained P–C bonds between the phosphite and COT groups. Precedence for this type of compound is found in the literature.

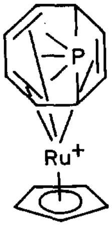

Nucleophilic attack of phosphines and phosphite on metal coordinated unsaturated systems is well documented [3,4]. In the resulting complexes, the phosphite or phosphine ligand is bound to either one or two additional carbon atoms of the unsaturated ring to form new P^V species. The resulting metal complexes exhibit altered ^1H, ^{13}C, and ^{31}P NMR spectra similar in many respects to those we obtain for $[(\eta^5-C_5H_5)Ru(\eta^4-COT)(P(OCH_3)_3)]PF_6$. Sweigart, in 1980, reported the formation of a new phosphonium adduct, $[(C_6H_6P(OCH_3)_3)(C_6H_6)Ru](PF_6)_2$, that results from trimethylphosphite attack at a η^6-benzene ring [5]. The doublet centered at 4.10 ppm, attributable to the phosphite methyl resonance in this compound, is shifted upfield approximately 0.5 ppm.

Herein, we report the X-ray crystal structure of $[(\eta^5-C_5H_5)Ru(\eta^4-COT)(P(OCH_3)_3]PF_6$ and an extensive study of the ^1H, ^{13}C, and ^{31}P NMR spectra of $[(\eta^5-C_5H_5)Ru(\eta^4-COT)(P(OCH_3)_3)]PF_6$ and the model compounds $[(\eta^5-C_5H_5)Ru(\eta^4-COT)(CO)]PF_6$, $[(\eta^5-C_5H_5)Ru(\eta^6-COT)]PF_6$ and $[(\eta^5-C_5H_5)Ru(\eta^4-COD)(P(OCH_3)_3)]PF_6$ (COD = 1,5-cyclooctadiene).

Experimental

General considerations

The following compounds used in syntheses and spectroscopic studies were prepared by literature methods: $[(\eta^5-C_5H_5)Ru-(\eta^6-C_6H_6)]PF_6$ [6], $[(\eta^5-C_5H_5)Ru-(P(OCH_3)_3)_3]PF_6$ [1], $[(\eta^5-C_5H_5)Ru(CH_3CN)_2(P(OCH_3)_3)]PF_6$ [1], $[(\eta^5-$

$C_5H_5)Ru(\eta^4\text{-COT})(CO)]PF_6$ [1] and $[(\eta^5\text{-}C_5H_5)Ru(\eta^6\text{-COT})]PF_6$ [1]. Cyclooctatetraene and 1,5-cyclooctadiene were purchased from Aldrich Chemical Co., Inc. The cyclooctatetraene was purified before use by passage through a short alumina column. The 1,5-cyclooctadiene was used without further purification. Spectroscopic grade dichloroethane was dried over alumina before use. All other reagents were used without further purification. Small scale synthetic photolyses were performed at 20 ° C in a quartz test tube equipped with a magnetic stir bar and serum stopper. The unfiltered output of a 175 W medium pressure mercury lamp was used as a light source. All solutions were degassed before photolysis or heating by bubbling them with nitrogen for approximately 15 min. The elemental analyses were performed by M-H-W Laboratories of Phoenix, Arizona.

High field ^1H NMR spectra (300 MHz), ^{31}P NMR spectra (121.5 MHz) and ^{31}C NMR spectra (75.461 MHz) were recorded on a Nicolet NT-300MHz WB instrument. ^1H and ^{13}C chemical shifts were internally referenced to tetramethylsilane. Phosphorus chemical shifts were referenced to external 85% orthophosphoric acid. Simulations of the spectra were accomplished using a program provided with the spectrometer. Simulations were optimized by comparison of the calculated values of the intensities and positions of individual peaks with those obtained experimentally. In a typical simulation, spectra were calculated in two parts of seven spins each.

Synthesis

$[(\eta^5\text{-}C_5H_5)Ru(\eta^4\text{-COT})(P(OCH_3)_3)]PF_6$

$[(\eta^5\text{-}C_5H_5)Ru(CH_3CN)_2(P(OCH_3)_3)]PF_6$ (171.5 mg) and 1.5 ml of cyclooctatetraene were dissolved in 15 ml of dichloroethane. This solution was refluxed under nitrogen for 23 h. The solvent was removed by rotary evaporation to yield a brown oil. This oil was washed with ether and hexane to remove unreacted cyclooctatetraene. The remaining oil was dissolved in dichloroethane and eluted down a short alumina column. The solvent was removed by rotary evaporation yielding 114.1 mg of yellow crystalline $[(\eta^5\text{-}C_5H_5)Ru(\eta^4\text{-COT})P(OCH_3)_3]PF_6$ (yield 64%). M.p. 116–118 ° C with decomposition. Anal. Found: C, 35.76; H, 4.14. $C_{16}H_{22}F_6O_3P_2Ru$ calc: C, 35.63; H, 4.11%.

$[(\eta^5\text{-}C_5H_5)Ru(\eta^4\text{-}C_8H_{12})(P(OCH_3)_3)]PF_6$

A 1.0 ml (8.15 mmol) sample of 1,5-cyclooctadiene was added to 65.9 mg (0.127 mmol) of $[(\eta^5\text{-}C_5H_5)Ru(CH_3CN)_2(P(OCH_3)_3)]PF_6$ in approximately 15 ml of dichloroethane. This solution was refluxed under nitrogen for approximately 20 h. The solvent was removed by rotary evaporation, after which the product was washed with hexane several times to remove unreacted 1,5-cyclooctadiene. Recrystalization from acetone/diethyl ether yielded 57.9 mg of yellow crystalline $[(\eta^5\text{-}C_5H_5)Ru(\eta^4\text{-COD})(P(OCH_3)_3)]PF_6$ (84% yield). Mp 208–210 ° C (with decomposition). Anal. Found: C, 35.49; H, 4.81. $C_{16}H_{26}F_6O_3P2Ru$ calc: C, 35.37; H, 4.82%.

X-Ray crystal structure determination of $[(\eta^5\text{-}C_5H_5)Ru(\eta^4\text{-COT})(P(CH_3)_3)PF_6$

Yellow crystals suitable for single crystal X-ray diffraction studies were grown from dichloromethane/ether solutions. The crystal selected for study was a parallelpiped of approximate dimensions 0.1 × 0.1 × 0.4 mm. This crystal was mounted

TABLE 1. CRYSTALLOGRAPHIC DATA AND COLLECTION PARAMETERS

Compound	$[(\eta^5\text{-}C_5H_5)Ru(\eta^4\text{-}COT)(P(OCH_3)_3)]PF_6$
Formula	$C_{16}H_{22}F_6O_3P_2Ru$
Formula wt.	539.4
Temperature	25 ° C
Space group	$P2_1$, no. 4
a (Å)	11.007(3)
b (Å)	11.066(3)
c (Å)	8.660(3)
β (°)	105.56
V (Å^3)	1016(1)
Z	2
d (calcd) (g cm^{-3})	1.763
d(obsd) (g cm^{-3})	1.73(1)
Cryst size (mm)	0.1 × 0.1 × 0.4
μ (cm^{-1})	9.864
Radiation (graphite-monochromated)	Mo-K_α (λ 0.71073 Å)
Scan type	$\omega-2\theta$
Scan width ($\Delta\omega$)	$0.70+0.35\tan(\theta)$
Collection range (°)	$2\theta = 0\text{–}54°$
Octants collected	$\pm h,k,l$
No. of unique data	3287
No. of data for $I > \sigma(I)$	2395
p	0.04
No. of variables	289
R_1	0.027 unweighted
R_2	0.031 weighted

on the end of a glass fiber with epoxy. The automatic peak searching, centering, and indexing routines available on the Enraf–Nonius SDP-CAD4 automatic diffractometer [7] were used to find and center 25 reflections that were used to determine the unit cell constants. The space group $P2_1$ was assigned by examining the data for systematic absences and was subsequently used successfully to solve and refine the structure. A summary of the crystal data and the collecting parameters used are given in Table 1. The density (ρ 1.73 g/cm^3) measured by the flotation method in aqueous $ZnCl_2$ solution is in agreement with the calculated value of 1.76 g/cm^3. A total of 3287 independent reflections was collected employing the ω–2θ scan technique in the scan range of $2\theta = 0\text{–}54°$ using graphite-monochromatized Mo-K_α radiation. Crystal decomposition was monitored by three check reflections. No decay or significant fluctuation in the intensities of these reflections was observed during data collection. After data processing and reduction [8], 2395 reflections for which $F_o^2 > \sigma(F_o^2)$ were used in the structure solution and refinement. No correction was made for absorption (μ 9.864 cm^{-1}).

The structure was solved from the three-dimensional Patterson function which allowed placement of the Ru atom and both P atoms. Fourier and difference Fourier analyses in conjunction with cycles of least-squares refinements [9] allowed the placement of the remaining non-hydrogen atoms. Full-matrix least-squares refinement utilizing anisotropic temperature factors for Ru, C, F, O and P (289 variables), and idealized placement of H atoms with temperature factors (B) fixed at 8.0 for the $C_5H_5^-$ and C_8H_8 hydrogens and 10.0 for the methyl hydrogens of the $P(OCH_3)_3$ ligand converged to give R and R_w of 0.027 and 0.031, respectively. Scattering factors were from Cromer and Waber [10]; the effects of anomalous dispersion were included [11]. The error in an observation of unit weight was 1.088, based on a value of 0.04 for ρ in the $\sigma(I)$ equation [8].

Disorder was observed in the PF_6^- anion. The positional and thermal parameters of the P atom and two *trans* F atoms (F(1) and F(2)) are well defined and yield expected bond lengths and bond angles; however, eight electron density peaks were found in the plane perpendicular to the F(1)–P–F(2) vector by examination of Fourier maps. These eight peaks were assigned to F atoms 3 through 10. Each of these F atoms were assigned a fixed occupancy factor of 0.5. Subsequent refinement followed by examination of a difference Fourier map suggested this disorder model to adequately model the electron density in this region of the unit cell.

Crystallographic and collection data are in Table 1. Final positional parameters are listed in Table 2. Selected bond distances and angles are given in Table 3.

TABLE 2

POSITIONAL PARAMETERS AND THEIR ESTIMATED STANDARD DEVIATIONS

Atom	x	y	z
Ru	0.18108(2)	0.2500(0)	0.25509(3)
P(1)	0.2591(1)	0.4208(1)	0.4005(1)
P(2)	−0.3353(1)	0.2911(2)	0.0142(2)
F(1)	0.7405(3)	0.1691(4)	0.0082(5)
F(2)	0.5923(4)	0.4127(4)	0.0227(6)
F(3)	0.3452(9)	−0.1710(9)	1.1562(10)
F(4)	0.6758(9)	0.2623(11)	0.1978(9)
F(5)	0.4564(6)	−0.2849(12)	1.0240(13)
F(6)	−0.2056(8)	0.3625(8)	0.0833(18)
F(7)	−0.2388(8)	0.3510(8)	−0.0604(13)
F(8)	−0.4398(7)	0.2366(14)	0.0666(13)
F(9)	−0.4192(8)	0.2538(13)	−0.1618(11)
F(10)	−0.2645(9)	0.3071(11)	0.1827(12)
O(1)	0.4010(4)	0.4548(4)	0.4128(5)
O(2)	0.1816(4)	0.5324(3)	0.3085(5)
O(3)	0.2478(4)	0.4447(4)	0.5741(4)
C(1)	0.4821(6)	0.4197(8)	0.3347(9)
C(2)	0.2057(8)	0.6541(6)	0.3699(8)
C(3)	0.3492(7)	0.4605(8)	0.7186(7)
CT(1)	0.0655(3)	0.2502(8)	0.4410(4)
CT(2)	0.0184(5)	0.1637(5)	0.3210(6)
CT(3)	0.0467(6)	0.0345(5)	0.3455(7)
CT(4)	0.1600(7)	−0.0074(5)	0.3634(8)
CT(5)	0.2655(5)	0.0756(5)	0.3537(6)
CT(6)	0.3134(5)	0.1590(5)	0.4742(7)
CT(7)	0.2620(6)	0.1701(5)	0.6147(6)
CT(8)	0.1480(6)	0.2113(5)	0.5983(6)
CP(1)	0.2630(4)	0.2463(8)	0.0476(5)
CP(2)	0.1684(5)	0.1548(5)	0.0226(5)
CP(3)	0.0548(5)	0.2119(5)	0.0086(5)
CP(4)	0.0726(5)	0.3351(6)	0.0325(6)
CP(5)	0.2024(6)	0.3572(5)	0.0492(6)

TABLE 3. SELECTED INTERATOMIC DISTANCES (Å) AND ANGLES (°) WITH THEIR ESTIMATED STANDARD DEVIATIONS

Ru–CT(1)	2.304(4)	CT(1)–Ru–CT(2)	36.0(3)
Ru–CT(2)	2.234(5)	CT(5)–Ru–CT(6)	35.8(2)
Ru–C(12) [a]	2.157(5)	CP(1)–CP(2)–CP(3)	107.2(6)
Ru–CT(5)	2.211(7)	CP(2)–CP(3)–CP(4)	110.5(7)
Ru–CT(6)	2.292(5)	CP(3)–CP(4)–CP(5)	106.4(7)
Ru–C(56) [a]	2.143(5)	CP(4)–CP(5)–CP(1)	108.5(6)
Ru–CP(1)	2.217(4)	CP(5)–CP(1)–CP(2)	107.1(5)
Ru–CP(2)	2.243(6)	CT(1)–CT(2)–CT(3)	122.3(6)
Ru–CP(3)	2.253(7)	CT(2)–CT(3)–CT(4)	122.3(6)
Ru–CP(4)	2.190(6)	CT(3)–CT(4)–CT(5)	120.4(6)
Ru–CP(5)	2.206(7)	CT(4)–CT(5)–CT(6)	120.6(7)
Ru–CCP [b]	1.875(6)	CT(5)–CT(6)–CT(7)	121.5(6)
Ru–P(1)	2.306(2)	CT(6)–CT(7)–CT(8)	120.5(5)
P(1)–O(1)	1.568(4)	CT(7)–CT(8)–CT(1)	122.3(5)
P(1)–O(2)	1.589(5)	CT(8)–CT(1)–CT(2)	119.7(9)
P(1)–O(3)	1.565(4)	Ru–P(1A)–O(1)	118.3(5)
O(1)–C(1)	1.371(8)	Ru–P(1A)–O(2)	107.0(5)
O(2)–C(2)	1.446(8)	Ru–P(1A)–O(3)	123.3(5)
O(3)–C(3)	1.447(7)	O(1)–P(1A)–O(2)	104.9(4)
CP(1)–CP(2)	1.427(11)	O(2)–P(1A)–O(3)	100.4(4)
CP(2)–CP(3)	1.377(11)	O(1)–P(1A)–O(3)	100.4(4)
CP(3)–CP(4)	1.385(11)	C(12)–Ru–C(56)	82.7
CP(4)–CP(5)	1.418(11)	C(12)–Ru–CCP	126.0
CP(5)–CP(1)	1.399(13)	C(12)–Ru–P(1A)	96.7
CT(1)–CT(2)	1.405(10)	C(56)–Ru–CCP	128.1
CT(2)–CT(3)	1.468(9)	C(56)–Ru–P(1A)	98.6
CT(3)–CT(4)	1.300(10)	CCP–Ru–P(1A)	116.4
CT(4)–CT(5)	1.501(11)		
CT(5)–CT(6)	1.387(9)		
CT(6)–CT(7)	1.478(9)		
CT(7)–CT(8)	1.307(9)		
CT(8)–CT(1)	1.484(8)		

[a] Atoms C(12) and C(56) refer to fictitious atoms midway between the CT(1), CT(2) and CT(5), CT(6) pairs. These atoms help define the geometry at Ru in terms of monodentate ligand equivalents. [b] CCP is a fictitious atom at the $C_5H_5^-$ ring centroid.

Supplementary tables 1–4 include anisotropic thermal parameters, positional and thermal parameters for the hydrogen atoms, least-squares planes, selected dihedral angles and observed and calculated structure factors.

Results

General descriptions

X-Ray structure of $[(\eta^5\text{-}C_5H_5)Ru(\eta^4\text{-}COT)(P(OCH_3)_3)]PF_6$

The structure consists of discrete $[(\eta^5\text{-}C_5H_5)Ru(\eta^4\text{-}COT)(P(OCH_3)_3)]^+$ cations and PF_6^- anions. There are no interionic contacts which are shorter than those expected for the Van der Waals contact distances. An ORTEP view of the cation is shown in Fig. 1. The cation contains a $\eta^5\text{-}C_5H_5^-$ ligand, a "normal" $P(OCH_3)_3$ ligand, and a COT ligand bound in the familiar $\eta^{1,2,5,6}$ tetrahapto fashion with the

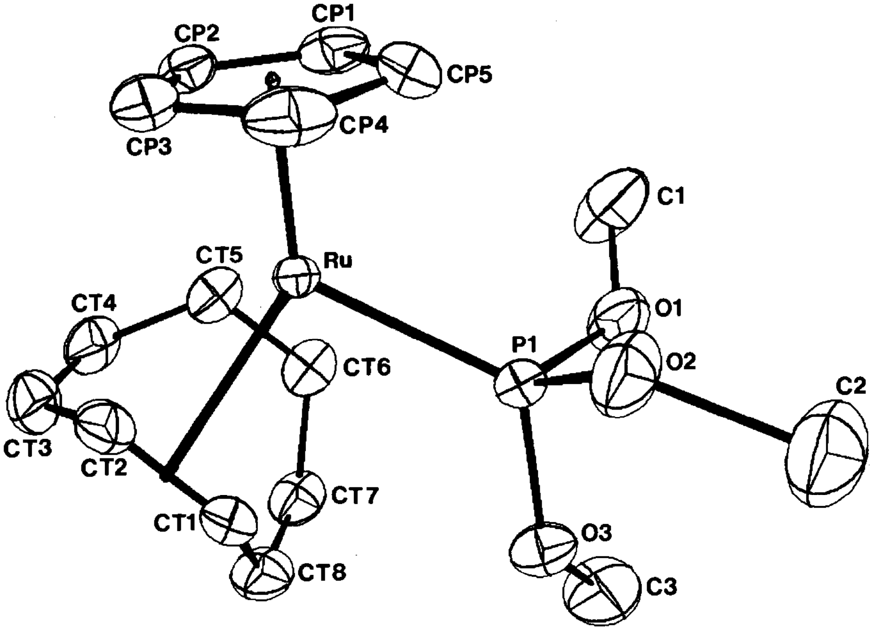

Fig. 1. ORTEP view of the $[(\eta^5\text{-}C_5H_5)Ru(\eta^4\text{-}COT)(P(OCH_3)_3)]^+$ cation. The thermal ellipsoids are drawn at the 50% level.

"tub" conformation. Of immediate interest, there is no indication of any bonding interactions between the P atom and any of the COT carbon atoms.

The coordination core approximates the "piano stool" type geometry commonly found for $(\eta^5\text{-}C_5H_5)ML_3$ and $(\eta^6\text{-}C_6H_6)ML_3$ structures with the $C_5H_5^-$ ligand occupying 3 coordination sites, C_8H_8 occupying 2 coordination sites and the $P(OCH_3)_3$ ligand occupying the sixth coordination site (see Tables and Fig. 1).

The Ru–C_5H_5 ring centroid distance of 1.875(5) Å and the average Ru–C distance of 2.221(7) Å are in good agreement with previously determined compounds. For example, 1.929 Å (Ru–ring centroid distance) in $[(\eta^5\text{-}C_5H_5)Ru(C_3Ph_2)(P(CH_3)_3)_2]PF_6$ [12], 2.170(6) Å (Ru–C) in $(\eta^5\text{-}C_5H_5)Ru(\eta^6\text{-}BPh_4)$ [13] and 2.24(1) Å (Ru–C) found for $(\eta^5\text{-}C_5H_5)Ru(C(CF_3C(H)C(CF_3)C_2CH(CF_3))(PPh_3)$ [14]. The $C_5H_5^-$ ring is closely planar, with the maximum deviation from planarity of 0.027 Å. The C–C bonds (av. 1.401(3) Å) within the $C_5H_5^-$ ring are also in good agreement with the other structures mentioned.

Two formal coordination sites are occupied by the $\eta^{1,2,5,6}$-COT moiety. (This analogy is best explored by defining two ficticious atoms (C(12) and C(56)) at the centers of the CT(1)–CT(2) and CT(5)–CT(6) carbon–carbon double bonds.) The Ru atom is bound to these two sets (CT(1), CT(6)) and (CT(2), CT(5)) of nearly chemically equivalent carbon atoms. The average Ru–C distances within these two sets are 2.298(5) and 2.223(6) Å. The difference between these sets (0.075 Å, ~ 13σ) is significant. To our knowledge, this structure appears to be the only structure of an η^4-COT complex determined to date in which this difference is significant. In the structure [15] of $(\eta^6\text{-}C_6H_6)Ru(\eta^4\text{-}1,5\text{-}COD)$ (COD = cyclooctadiene) which contains Ru^0, the four Ru–C bonds to the COD ligand are slightly shorter (2.138(5) Å) than the present Ru^{II} case and are identical within experimental error.

In the present case, the longer Ru–C bonds (Ru–CT(1) and Ru–CT(6)) probably result from repulsive interactions between the η^4-COT and the $P(OCH_3)_3$ ligands. This effect may also be reflected in the slight opening of the P(1)–Ru–C(12) and P(1)–Ru–C(56) angles (96.7 and 98.6°), respectively, from the 90° angles expected.

The "tub" shape conformation of the $\eta^{1,2,5,6}$-COT ligand produces an effective bite angle as defined by the C(12)–Ru–C(56) angle of 82.7(3)°. The COT ligand

TABLE 4. ^{1}H [a], ^{13}C [a], AND ^{31}P [b] NMR SUMMARY [c]

Atom(s) [d]	Simulation	Experiment
$[(\eta^5\text{-}C_5H_5)Ru(\eta^4\text{-}COT)(P(OCH_3)_3)]PF_6$		
H (η^5-$C_5H_5^-$)	–	5.54(s)
H(1,6)	4.33	4.33(d of d of d of d)
H(2,5)	5.31	5.31(d of d of d of d)
H(7,8)	6.07	6.07(d of d of d)
H(3,4)	5.97	5.97(d of d of d)
H ($P(OCH_3)_3$)	–	3.95(d)
C (η^5-$C_5H_5^-$)	–	88.24(d)
C(1,6)	–	84.01(d)
C(2,5)	–	82.89(s)
C(7,8)	–	133.56(d)
C(3,4)	–	136.71(s)
C($P(OCH_3)_3$)	–	55.23(d)
P($P(OCH_3)_3$)	–	163.63(s)
$[(\eta^5\text{-}C_5H_5)Ru(\eta^4\text{-}COD)(P(OCH_3)_3)]PF_6$		
H (η^5-$C_5H_5^-$)	–	5.17(s)
H(1,6)	–	4.06(m)
H(2,5)	–	4.88(m)
H(7,8)	–	1.91(m)
		2.26(m)
H(3,4)	–	2.06(m)
		2.35(m)
H ($P(OCH_3)_3$)	–	3.83(d)
C (η^5-$C_5H_5^-$)	–	86.69(s)
C(1,6)	–	79.73(d)
$[(\eta^5\text{-}C_5H_5)Ru(\eta^4\text{-}COD)(P(OCH_3)_3)]PF_6$		
C(2,5)	–	79.40(s)
C(7,8)	–	31.93(s)
C(3,4)	–	29.64(s)
C ($P(OCH_3)_3$)	–	54.26(d)
P ($P(OCH_3)_3$)	–	151.18(s)
$(\eta^5\text{-}C_5H_5)Ru(\eta^4\text{-}COT)(CO)]PF_6$		
H (η^5-$C_5H_5^-$)	–	5.87(s)
H(1,6)	5.19	5.19(d of d)
H(2,5)	5.79	5.79(d)
H(7,8)	6.06	6.06(d)
H(3,4)	6.38	6.38(s)
H ($P(OCH_3)_3$)	–	–
C (η^5-$C_5H_5^-$)	–	89.17(s)
C(1,6)	–	89.70(s) or
C(2,5)	–	91.92(s)
C(7,8)	–	134.13(s) or
C(3,4)	–	135.85(s)

TABLE 4 (continued)

Atom(s) [d]	Simulation	Experiment
$(\eta^5$-$C_5H_5)Ru(\eta^6$-$COT)]PF_6$ [e]		
H (η^5-$C_5H_5^-$)	–	5.75(s)
H(1,6)	6.02	6.02(d of d)
H(2,5)	6.10	6.10(d of d of d)
H(7,8)	5.15	5.15(d)
H(3,4)	6.98	6.98 (d of d)
$[(\eta^5$-$C_5H_5)Ru(P(OCH_3)_3)_3]PF_6$		
C (η^5-$C_5H_5^-$)	–	85.56 (q)
C ($P(OCH_3)_3$)	–	53.50 (q)
P ($P(OCH_3)_3$)	–	153.25 (s)

[a] ^1H and ^{13}C peak positions are internally referenced to tetramethylsilane. [b] ^{31}P peak positions are referenced to external 85% orthophosphoric acid and are proton decoupled. [c] All spectra were obtained on acetone d_6 solutions. [d] Numbering of atoms follows the scheme outlined in the text. [e] Numbering of the COT ring follows the same convention as for the other compounds, but C(3) and C(4) are also bound to the metal.

C–C single bonds of 1.48(1) Å and the C–C–C bond angles of 121(1)°, are close to the normal values expected. Comparison of the C–C–C bond angles in which carbon–ruthenium bonds occur and those in which carbon does not interact with ruthenium show no difference in bond angles. There is, however, a significant lengthening of the two double bonds coordinated to ruthenium (av. 1.40(1) Å) compared to the two carbon–carbon double bonds that are not coordinated (average 1.30(1) Å, 0.1 Å or 7σ difference). This lengthening of the carbon–carbon double bond on coordination is well documented. For example, in (η^6-C_6H_6)Ru(η^4-1,5-COD) the coordinated double bonds are reported as 1.403(8) Å. Previously this lengthening [16] has been ascribed to back-donation of electron density from the relatively electron rich metal center into the π^* MO of the carbon–carbon π bond.

The trimethyl phosphite ligand is bound to the Ru through an apparently normal Ru–P interaction (Ru–P(1) bond length of 2.306(2) Å). In comparison, the Ru–P bonds in $[(\eta^5$-$C_5H_5)Ru(C_3Ph_2)(P(CH_3)_3)_2]PF_6$ [12], $(\eta^5$-$C_5H_5)Ru(C(CF_3C$-$(H)C(CF_3)C_2CH(CF_3))(PPh_3)$ [14], $(\eta^6$-$C_6H_6)Ru(Cl)_2(P(CH_3)(Ph)_2)$ [17] and $(\eta^6$-p-$CH_3C_6H_4CH(CH_3)_2)Ru(Cl)_2(P(CH_3)Ph)_2)$ are 2.291, 2.335, 2.335 and 2.341 Å, respectively.

Although there are no close contacts indicated between the trimethyl phosphite ligand and the CT(7) and CT(8) portion of the COT ligand, there appears to be asymmetry in the Ru–P–O bond angles, of 118.3(5), 107.0(5) and 123.3(5)°, respectively, for O = O(1), O(2) and O(3). This asymmetry is likely due to a steric interaction of the oxygens and methyl groups with the CT(7) and CT(8) region of the COT ligand. The O–P(1)–O angles are also influenced by this interaction, with values of O(1)–P(1A)–O2, O2–P(1A)–O3 and O1–P(1A)–O3 of 104.9(4), 100.4(4) and 100.4(4)°, respectively.

NMR spectral results

^1H, ^{31}P, and ^{13}C NMR spectra were recorded and analyzed for the four compounds $[(\eta^5$-$C_5H_5)Ru(\eta^4$-$COT)(P(OCH_3)_3)]PF_6$, $[(\eta^5$-$C_5H_5)Ru(\eta^4$-$COD)(P$-$(OCH_3)_3)]PF_6$, $[(\eta^5$-$C_5H_5)Ru(\eta^4$-$COT)(CO)]PF_6$, and $[(\eta^5$-$C_5H_5)Ru(\eta^6$-$COT)]PF_6$.

^{31}P decoupled proton spectra were also recorded for $[(\eta^5\text{-}C_5H_5)Ru(\eta^4\text{-}COT)(P(OCH_3)_3)]PF_6$ as well as ^{13}C and ^{31}P NMR spectra of $[(\eta^5\text{-}C_5H_5)Ru(P(OCH_3)_3)_3]PF_6$. The results of these studies and simulations of the spectra are outlined for individual compounds below. Discussion of the spectra follows in the next section. Table 4 summarizes the peak positions for all compounds. The assignment of peaks was accomplished through decoupling experiments, simulations and through comparisons with previously assigned organic and organometallic compounds [18–21]. The numbering scheme that is used for the COT and COD framework is shown below.

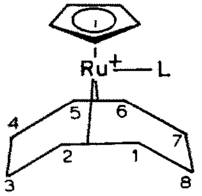

$[(\eta^5\text{-}C_5H_5)Ru(\eta^4\text{-}COT)(P(OCH_3)_3)]PF_6$. The 300 MHz ^1H NMR spectrum of this compound consists of three main sets of peaks: one due to the cyclopentadienyl ligand, one assigned to the trimethylphosphite ligand methyl protons and one to the cyclooctatetraene ligand. The cyclopentadienyl ligand resonates as a singlet at 5.54 ppm rather than the expected doublet for a structure that contains a phosphite bound directly to the ruthenium metal center. The trimethylphosphite doublet appears at 3.95 ppm (J(P–H) 11.3 Hz), shifted slightly upfield from compounds of similar structure [1,2]. The plane of symmetry bisecting the cyclopentadienyl and cyclooctatetraene rings requires the COT proton resonances to split into four distinct sets of two protons each. A complex pattern at 4.3 ppm is resolved into a doublet of doublets of doublets of doublets which overlap to give a symmetrical 11 line pattern. The upfield shift of this signal and the large J(P–H) coupling constant (11.4 Hz) is constant with its assignment to protons one and six (the two carbons coordinated to ruthenium and nearest the phosphite). The protons at positions 2 and 5 are also shifted considerably upfield from the free ligand and likewise appear as a doublet of doublets of doublets of doublets. The smaller J(P–H) of 1.1 Hz in this case results in a doublet for line patterns. The remaining four COT protons resonate as two doublets of doublets of doublets. The peak at 5.97 ppm, assigned to H(3,4), is split into a four line pattern of overlapping doublets and has a J(P–H) 1.1 Hz, while that ascribable to H(7,8) is split into a five-line pattern centered at 6.07 ppm with a J(P–H) 2.5 Hz. The slightly larger J(P–H) observed for these protons is presumably a result of the closer proximity of the phosphite ligand (see Discussion which follows). As is the case for the remainder of the compounds, many of the coupling constants observed in the spectrum of $[(\eta^5\text{-}C_5H_5)Ru(\eta^4\text{-}COT)(P(OCH_3)_3)]PF_6$ are equivalent within experimental error. The ^1H COT assignments for this compound were confirmed through results obtained from a ^{31}P decoupled proton spectrum which allowed the unambiguous evaluation of the J(P–H) values. Coupling constants obtained from simulations of the ^1H NMR spectra are as follows: $J_{1,2} = J_{5,6} = 8.88$ Hz; $J_{1,7} = J_{1,8} = J_{6,7} = J_{6,8} = 1.3$ Hz; $J_{2,3} = J_{2,4} = J_{3,5} = J_{4,5} = 1.1$ Hz. Experimental and simulated spectra of the COT resonances from the undecoupled and ^{31}P decoupled ^1H NMR experiments are shown in Fig. 2.

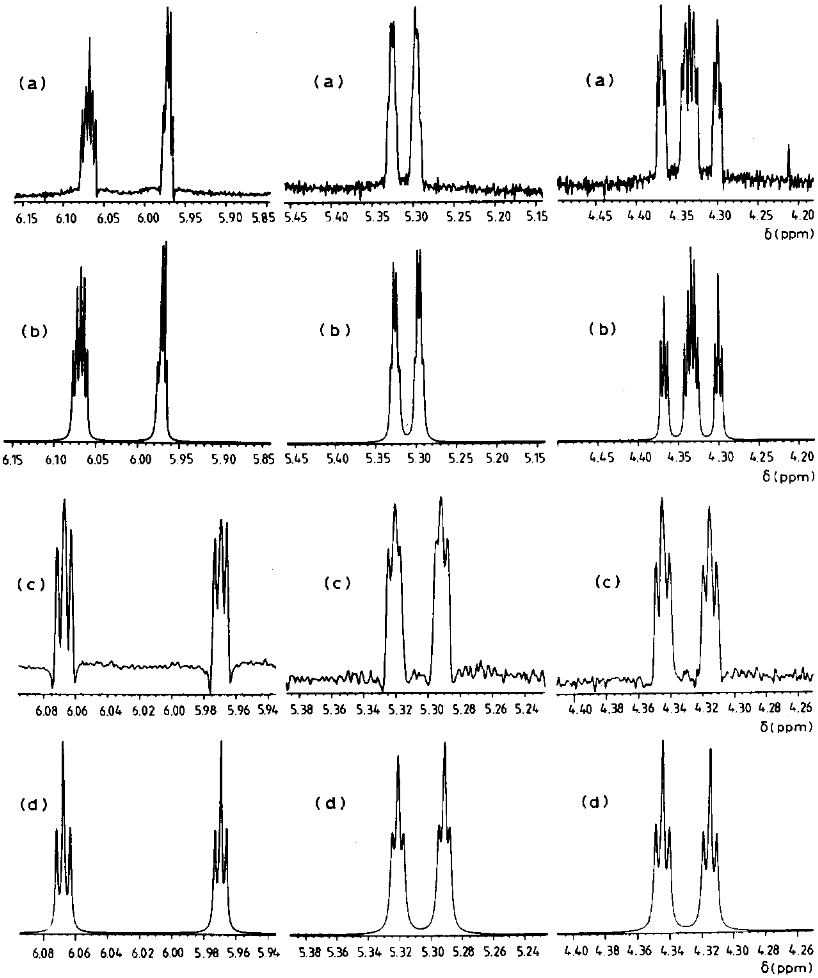

Fig. 2. ^{1}H NMR spectra of the COT resonances of $[(\eta^5\text{-}C_5H_5)Ru(\eta^4\text{-COT})(P(COH_3)_3)]PF_6$. From left to right are exhibited expansions of the signals due to H(1,6), H(2,5) and H(3,4,7,8), respectively. Curves labeled (a) and (b) are undecoupled spectra. Curves labeled (c) and (d) are ^{31}P decoupled. Curves (a) and (c) are experimental spectra while curves (b) and (d) are simulations.

A ^{1}H decoupled ^{13}C NMR spectrum of the compound was also recorded. A doublet of intensity 3 at 55.23 ppm with a $^{13}C\text{–}^{31}P$ coupling constant of 8.21 Hz is assigned to the trimethylphosphite carbon atoms. The cyclopentadienyl ring carbons resonate at 88.24 ppm and appear as a doublet split by the phosphorus with a coupling of only 0.93 Hz. The eight COT carbons resonate as 4 signals in two distinct regions of the spectrum. The four carbons directly bound to the metal are observed at 82.89 ppm (s) and 84.01 ppm (d, *J*(P–C) 6.96 Hz). The exact assignment of one of these resonances to the carbons closest to the phosphorus atom is difficult because the angles that determine the magnitude of the $^{31}P\text{–}^{13}C$ coupling are similar for both sets of carbons. Tentatively, we assign carbons one and six to the doublet at 84.01 ppm. The carbons at positions two and five are then assigned to the peak at 82.89 ppm. The uncoordinated carbon resonances occur at 133.56 ppm (d, J(P–C) 1.70 Hz) and at 136.71 (s). Consistent with the previous assignment, the resonance at 133.56 ppm that exhibits ^{31}P–^{13}C coupling, is assigned to carbons 7 and 8 and the singlet at 136.71 ppm is assigned to carbons three and four.

The proton decoupled ^{31}P NMR spectra of $[(\eta^5\text{-}C_5H_5)Ru(\eta^4\text{-}COT)(P(OCH_3)_3)]PF_6$ consists of a singlet at 163.63 ppm, while the undecoupled ^{31}P spectrum consists of a complex pattern of at least eight lines.

$[(\eta^5\text{-}C_5H_5)Ru(\eta^4\text{-}COD)(P(OCH_3)_3)]PF_6$. The non-equivalence of the protons attached to the saturated carbons of the 1,5-cyclooctadiene ligand result in a complicated ^{1}H NMR spectrum for $[(\eta^5\text{-}C_5H_5)Ru(\eta^4\text{-}COD)(P(OCH_3)_3)]PF_6$ that was not simulated, but assignment of sets of resonances to specific protons was possible. The cyclopentadienyl resonance is a singlet at 5.17 ppm. The phosphite methyl group protons appear as the expected doublet at 3.83 ppm with a coupling constant J(P–H) of 11.5 Hz. The protons associated with the carbons directly bound to the ruthenium occur as two sets of two protons each shifted upfield from the uncoordinated ligand. Each set of equivalent saturated carbons has two sets of two equivalents protons bound to them. Each of these is observed as four unresolvable multiplets between 1 and 3 ppm (see Fig. 3). Both proton and phosphorus decoupled ^{1}H spectra were recorded to aid in assignment of these peaks. ^{31}P decoupling leads to significant changes only in the multiplet centered at 4.06 ppm. ^{1}H decoupling at the frequency of the protons at 4.8 Hz causes the 4.06 ppm multiplet to collapse to a multiplet from which a J(P–H) of 12.6 Hz is abstracted. The large J(P–H) coupling constant for this peak suggests its assignment to the two protons at the one and six position. By default, H(2,5) is assigned to the multiplet centered at 4.88 ppm. While no significant changes were observed in the saturated hydrogen region of the spectrum in the ^{31}P decoupled ^{1}H spectrum, saturated hydrogen resonances did simplify somewhat upon decoupling of the H(2,5) and H(1,6) protons. Irradiation at the frequency of protons 1 and 6 (4.0 ppm) caused the multiplets centered at 1.91 and 2.26 ppm to collapse. These signals are therefore assigned to the four hydrogens bound to carbons seven and eight. Irradiation at 4.8 ppm led to the collapse of the peaks centered at 2.06 and 2.35 ppm. These are assigned to the four protons at positions three and four.

The ^{1}H decoupled ^{13}C NMR spectrum of $[(\eta^5\text{-}C_5H_5)Ru(\eta^4\text{-}COD)(P(OCH_3)_3)]PF_6$ consists of six resonances. The phosphite methyl carbons are assigned to the doublet at 54.26 ppm which has a J(P–C) of 7.5 Hz. In contrast to the spectrum of $[(\eta^5\text{-}C_5H_5)Ru(\eta^4\text{-}COT)(P(OCH_3)_3)]PF_6$, that exhibits a phosphorus coupled doublet for the cyclopentadienyl carbons, the cyclopentadienyl ligand resonance in $[(\eta^5\text{-}C_5H_5)Ru(\eta^4\text{-}COD)(P(OCH_3)_3)]PF_6$ is a singlet of intensity five at 86.69 ppm. The coordinated COT carbons at positions one and six resonate as a doublet at 79.73 ppm (J(P–C) 8.03 Hz) and those at positions two and five appear at 79.40 ppm as a singlet. The two remaining singlets at 29.64 and 31.93 ppm are assigned to the uncoordinated carbon resonances.

The ^{1}H decoupled ^{31}P spectrum consists of a singlet assigned to the phosphite phosphorus at 151.12 ppm relative to phosphoric acid external standard.

$[(\eta^5\text{-}C_5H_5)Ru(\eta^4\text{-}COT)(CO)]PF_6$. The substitution of the trimethylphosphite ligand in $[(\eta^5\text{-}C_5H_5)Ru(\eta^4\text{-}COT)(P(OCH_3)_3)]PF_6$ with a ligand that does not introduce additional coupling constants into the remainder of the resonance greatly

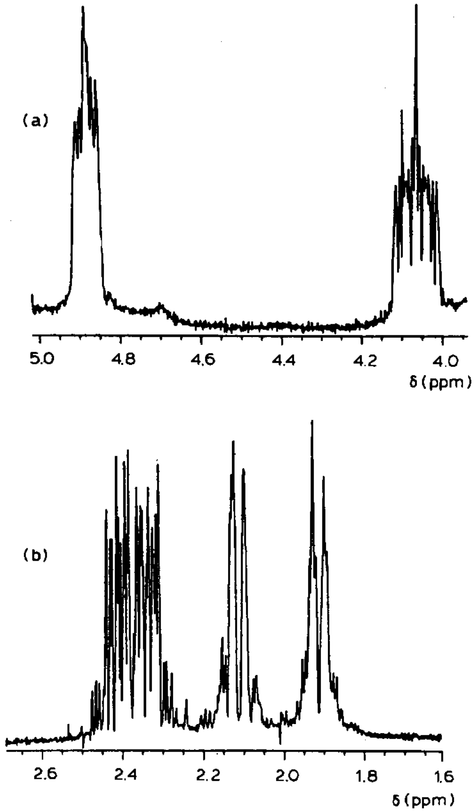

Fig. 3. ^1H NMR spectra of the COD resonances of $[(\eta^5\text{-}C_5H_5)Ru(\eta^4\text{-}COD)(P(OCH_3)_3]PF_6$. Curve (a) and curve (b) are expansions for the H(1,2,5,6) and H(3,4,7,8) signals, respectively.

simplifies the COT portion of the ^1H NMR spectrum of this complex. A peak of intensity five at 5.874 ppm is assigned to the cyclopentadienyl ligand bound to the metal. As in the case of the complex $[(\eta^5\text{-}C_5H_5)Ru(\eta^4\text{-}COT)(P(OCH_3)_3)]PF_6$, symmetry requires that the coordinated COT protons split into four sets of two protons. These are assigned to specific resonances by comparison with the spectrum of $[(\eta^5\text{-}C_5H_5)Ru(\eta^4\text{-}COT)(P(OCH_3)_3)]PF_6$. A doublet of doublets centered at 5.19 ppm and a doublet at 5.79 ppm are assigned to H(1,6) and H(2,5) respectively. The proton signal for H(7,8) is split into a doublet at 6.06 ppm, but surprisingly the signal for H(3,4) appears as a singlet at 6.38 ppm. H(3,4) shows no coupling with any of the other protons in the molecule. Simulation of the spectrum revealed the following coupling constants: $J_{1,2} = J_{5,6} = 8.66$ Hz; $J_{1,8} = J_{6,7} = 0.9$ Hz.

The ^1H decoupled ^{13}C spectrum of $[(\eta^5\text{-}C_5H_5)Ru(\eta^4\text{-}C_8H_8)(CO)]PF_6$ is simple. It consists of five singlets. The singlet due to the cyclopentadienyl carbons is observed at 89.17 ppm. The four carbons bound to the ruthenium appear as singlets at 89.70 and 91.92 ppm while the four carbons that are not bound to Ru resonate at 134.13 and 135.85 ppm. The carbon resonance of the CO ligand was not recorded.

$[(\eta^5\text{-}C_5H_5)Ru(\eta^6\text{-}COT)]PF_6$. The ^1H NMR spectrum of $[(\eta^5\text{-}C_5H_5)Ru(\eta^6\text{-}COT)]PF_6$ was recorded for comparison to the η^4-bound compounds. Binding of the

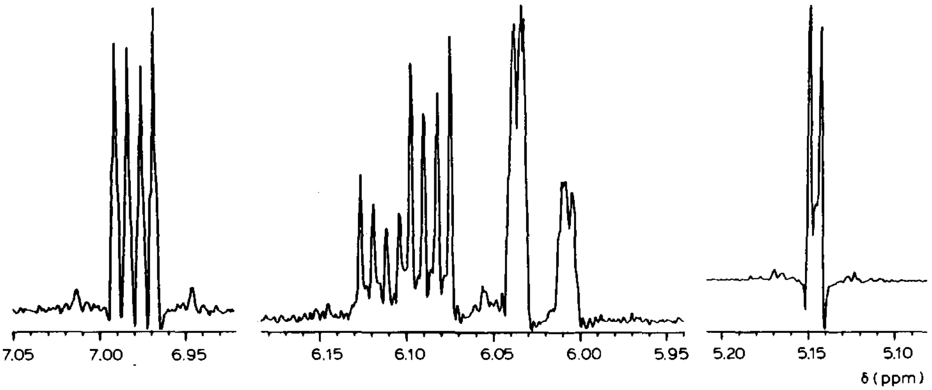

Fig. 4. ^1H NMR spectra of the COT resonances of $[(\eta^5\text{-}C_5H_5)Ru(\eta^6\text{-}COT)]PF_6$.

COT ring in this compound occurs through carbons one through six with the unbound carbons 7 and 8 presumably *exo* to the C(1–6) plane of the molecule. The proton spectrum is unexceptional; the cyclopentadienyl ring resonance occurs at 5.75 ppm and the COT protons resonate as four sets of two protons each. The signal from the hydrogens at positions 2 and 5 appear as a doublet of doublets of doublets at 6.10 ppm while H(1,6) and H(3,4) are both split into doublet of doublets at 6.02 and 6.98 ppm, respectively. The hydrogens on the unbound carbons at positions 7 and 8 are shifted 0.49 ppm upfield from those in the free COT and appear as a doublet at 5.15 ppm. As expected, ^1H decoupling at 5.1 ppm led to the collapse of the peak at 6.02 ppm whereas decoupling at 6.9 ppm collapsed the peak centered at 6.10 ppm. Simulations of the ^1H spectrum were successful with the following set of coupling constants: $J_{1,8} = J_{6,7} = 1.6$ Hz; $J_{1,2} = J_{5,6} = 8.0$ Hz; $J_{2,3} = J_{4,5} = 4.6$ Hz; $J_{2,4} = J_{3,5} = 2.2$ Hz. Enlargements of the portion of the spectrum showing the COT resonances are shown in Fig. 4.

$[(\eta^5\text{-}C_5H_5)Ru(P(OCH_3)_3)_3]PF_6$. The ^1H decoupled ^{13}C NMR spectrum of $[(\eta^5\text{-}C_5H_5Ru(P(OCH_3)_3)_3]PF_6$ was recorded for comparison with spectra of the complexes of interest. The compound exhibits two peaks, a quartet at 85.56 ppm ascribable to the cyclopentadienyl carbons (J(C–P) 2.4 Hz), and another quartet at 53.50 ppm (J(C–P) 2.4 Hz) assigned to the methyl carbons of the trimethylphosphite.

Discussion

Complete NMR spectral studies (^1H, ^{13}C, ^{31}P) prove that $[(\eta^5\text{-}C_5H_5)Ru(\eta^4\text{-}COT)(P(OCH_3)_3)]PF_6$ does not adopt an unconventional formulation in solution. The most direct evidence arises from the similarity of the ^1H NMR spectra of the complex $[(\eta^5\text{-}C_5H_5)Ru(\eta^4\text{-}COD)(P(OCH_3)_3)]PF_6$ to that of $[(\eta^5\text{-}C_5H_5)Ru(\eta^4\text{-}COT)(P(OCH_3)_3)]PF_6$. The ^1H NMR of the model compound, $[(\eta^5\text{-}C_5H_5)Ru(\eta^4\text{-}COD)(P(OCH_3)_3)]PF_6$ displays the three characteristics that placed the solution structure of $[(\eta^5\text{-}C_5H_5Ru(\eta^4\text{-}COT)(P(OCH_3)_3)]PF_6$ in doubt even though the COD complex is only capable of the conventional formulation. The cyclopentadienyl resonance is a singlet that is not coupled to the coordinated phosphite, the phosphite methyl resonance is 0.1 ppm downfield from its expected position and the peaks ascribable to the COD protons are complex enough to ensure the precence of large P–H coupling. Because there are C–C single bonds between carbons 7,8 and 3,4, the COD complex is only able to adopt the conventional tub configuration with direct coordination of the phosphite to the ruthenium. Thus the similarity of the spectra obtained for the COD and COT compounds ensures that the solid state structure of the COT compound persists in solution. ^{13}C data collected for these two complexes and the similar $[(\eta^5\text{-}C_5H_5)Ru(\eta^4\text{-}COT)(CO)]PF_6$ compound are also consistent with normal Ru–P coordination in $[(\eta^5\text{-}C_5H_5)Ru(\eta^4\text{-}COT)(P(OCH_3)_3)]PF_6$. If carbons of the COT ring in $[(\eta^5\text{-}C_5H_5)Ru(\eta^4\text{-}COT)(P(OCH_3)_3)]PF_6$ were bound to the phosphorous atom, peaks exhibiting significant ^{31}P–^{13}C coupling, would have been evident in the ^{13}C spectrum. In contrast, all three complexes have resonances for C(1,6) and C(2,5) that fall in the range 79 to 89 ppm. Additionally, the phosphite methyl carbons of both $[(\eta^5\text{-}C_5H_5)Ru(\eta^4\text{-}COT)(P(OCH_3)_3)]PF_6$ and $[(\eta^5\text{-}C_5H_5)Ru(\eta^4\text{-}COD)(P(OCH_3)_3)PF_6$ resonate at 55.225 and 54.255 ppm, respectively, in agreement with the position of 53.501 ppm observed for $[(\eta^5\text{-}C_5H_5)Ru(P(OCH_3)_3)_3]PF_6$, a compound known to have Ru–P bonds. These results confirm that the solution structure and the crystal structure of $[(\eta^5\text{-}C_5H_5)Ru(\eta^4\text{-}COT)(P(OCH_3)_3)]PF_6$ are identical.

Although simulations of the spectra were not required to assign the solution structure of $[(\eta^5\text{-}C_5H_5)Ru(\eta^4\text{-}COT)(P(OCH_3)_3)]PF_6$ the complexity fo the ^{1}H NMR data remained a mystery. We reasoned that the symmetry plane that passes through the cyclopentadienyl ring, the phosphorous atom and the cyclooctatetraene ring required the protons of the COT ring to split into 4 equivalent sets of two protons each, with a simple splitting pattern. Instead, an apparent quintet, a pseudo quartet, a pseudo doublet of quartets and a pseudo doublet of doublet of triplets is observed in the spectrum. Computer simulations were utilized to unravel the complexity of the spectrum. These simulations indicate that the best fit of the experimental data occurs only for simulations that allow all the COT ring protons to couple to the phosphite phosphorus atom. A ^{31}P decoupled ^{1}H NMR experiment was carried out to confirm this hypothesis. In this case, all peaks assigned to the COT moiety collapse to overlapping doublets of doublets, the result of one remaining vicinal coupling and one allylic coupling. With the vicinal and allylic ^{1}H–^{1}H couplings revealed, the simulations of both the undecoupled and ^{31}P decoupled experiments were refined to obtain consistent values for the coupling constants and peak positions (vide supra). We note that the angular relationship between the phosphite phosphorus and protons 1,6 and protons 2,5 is roughly the same as a vicinal, ^3J type ^{1}H–^{1}H coupling. Theoretical considerations predict that differences in the magnitude of vicinal ^3J coupling depend on the dihedral and vicinal angles of the molecular framework [22]. By employing the equations designed for hydrocarbon systems, both the dihedral and vicinal dependence of ^3J predicts that $J_{1,6\text{-P}} > J_{2,5\text{-P}}$, consistent with experiment. Assignment of the H(7,8) and H(3,4) resonances follows easily from additional proton–proton coupling constant information.

The observation of the extensive ^{31}P–^{1}H couplings between the phosphite and the cyclooctatetraene ring was unexpected, particularly with the lack of phosphorus coupling to the cyclopentadienyl ring ^{1}H resonance (a very small ^{31}P–^{13}C coupling constant (1.0 Hz) is observed in the ^{13}C spectrum). The couplings between the phosphorus and the protons bound to carbons 1,6 and 7,8 are particularly large;

11.4 Hz to H(1,6) and 2.5 Hz to H(7,8). The ^{31}P coupling to H(1,6) is comparable to those observed between phosphorus and the phosphite methyl protons and, in fact, is carried over the same number of bonds. However, the protons at positions 2 and 5 are the same number of bonds from the phosphorus but exhibit a $^{31}P-^{1}H$ coupling constant of only 1.08 Hz. Similarly the cyclopentadienyl ring protons have the same relationship to the phosphorus as H(2,5) and H(1,6) but show no coupling to the phosphite. Perhaps in this instance both the phosphite and the cyclooctatetraene are bound to the Ru in a configuration with the most fortuitous angles for strong coupling only to H(1,6). The magnitude of the coupling constant between the phosphorus and H(7,8) (J 2.4 Hz) is unusually large for atoms separated by four bonds [23]. Part of this effect may be a result of through space coupling enhanced by the steric interaction between these protons and the methyl groups of the phosphite ligand. Through space coupling may explain not only the magnitudes of $J_{7,8\text{-P}}$ and $J_{3,4\text{-P}}$, but also $J_{1,6\text{-P}}$ and $J_{2,5\text{-P}}$ if the phosphite-COT steric interaction increases J(HP) values for all of the protons on the 'phosphite side' of the complex.

The successful simulation of the ^{1}H NMR spectrum of $[(\eta^5\text{-}C_5H_5)Ru(\eta^4\text{-}COT)(P(OCH_3)_3)]PF_6$ also requires the presence of vicinal couplings between hydrogens on adjacent carbons in the COT ring and allylic couplings across the ring. The vicinal coupling constant between hydrogens attached to coordinated carbons is 8.9 Hz, well within the range expected for coupling through a carbon–carbon double bond of this type. The vicinal couplings between hydrogens on a carbon bound to the metal and hydrogens on an uncoordinated carbon are much smaller ($J_{1,8} = J_{6,7} = 1.3$ Hz and $J_{2,3} = J_{4,5} = 1.1$ Hz) but are in agreement with the theoretical predictions based on the larger dihedral angles indicated from the solid state structure (69 and 91°, respectively). The four allylic couplings derived from the simulations deviate significantly from predictions derived from organic examples. The experimental spectra can only be successfully simulated if the allylic coupling constants are positive. Theoretical considerations based on organic unsaturated systems predict small, negative allylic couplings. Perhaps in this example, the perturbation of the π system by coordination of the COT ring to the metal changes the π electron density sufficiently to invalidate the organic based equations.

Although the splitting pattern discernable in the ^{1}H NMR spectrum of $[(\eta^5\text{-}C_5H_5)Ru(\eta^4\text{-}COT)(CO)]PF_6$ is similar to that of $[(\eta^5\text{-}C_5H_5)(\eta^4\text{-}COT)(P(OCH_3)_3)]PF_6$ there are significant deviations. The better π-backbonding ability of the CO ligand in comparison to $P(OCH_3)_3$, causes H(1,6) and H(2,5) to be deshielded, (0.86 and 0.48 ppm further downfield, respectively) relative to those in the $P(OCH_3)_3$ compound. All vicinal couplings in the CO compound are smaller in magnitude and the allylic couplings are zero. We tentatively attribute this result to a decrease in the steric interaction between COT and CO that results in less favorable angles for large coupling constants. Alternatively, the CO ligand might withdraw sufficient electron density from the COT ring to decrease the transference of spin through the π system, with a concomitant decrease in the magnitude of the coupling constants in question.

The complex $[(\eta^5\text{-}C_5H_5)Ru(\eta^6\text{-}COT)]PF_6$ provides an example of the COT ring bound in a η^6 arrangement unperturbed by any additional ligands. Six of the eight carbons of the cyclooctatetraene are involved in Ru–COT bonding, with carbons 7 and 8 unbound and presumably bent in an *exo* conformation out of the plane of the ring. Again the protons of the COT ring resonate as four sets of two protons.

Significant proton coupling is observed between the allylic proton pairs 2 and 4, and 3 and 5. The magnitude of these coupling constants determined via the computer simulations, agree well in magnitude and sign with those of $[(\eta^5\text{-}C_5H_5)Ru(\eta^4\text{-}COT)(P(OCH_3)_3)]PF_6$ and $[(\eta^5\text{-}C_5H_5)Ru(\eta^4\text{-}COT)(CO)]PF_6$. The vicinal couplings that involve coordinated carbon atoms are 8.0 Hz carbon–carbon double bonds and 4.6 Hz (carbon–carbon single bonds). The vicinal coupling between the uncoordinated hydrogens, 7 and 8, is much smaller (1.6 Hz) and is similar to the values obtained for the analogous coupling in the tub configuration of the bound COT in $[(\eta^5\text{-}C_5H_5Ru(\eta^4\text{-}COT)(P(OCH_3)_3)]PF_6$ and $[(\eta^5\text{-}C_5H_5)Ru(\eta^4\text{-}COT)(CO)]PF_6$. The value of 2.2 Hz for the allylic couplings $J_{2,4}$ and $J_{3,5}$ extracted from the ^1H NMR simulation of $(\eta^5\text{-}C_5H_5)Ru(\eta^6\text{-}COT)^+$ suggests that positive allylic coupling constants are normal in these systems in contrast to those found in the uncoordinated organic system.

Although the spectra obtained for $[(\eta^5\text{-}C_5H_5)Ru(\eta^4\text{-}COD)(P(OCH_3)_3)]PF_6$ were useful for comparison with $[(\eta^5\text{-}C_5H_5)Ru(\eta^4\text{-}COT)(P(OCH_3)_3)]PF_6$ and in the solution structure determination, no easily obtainable information concerning proton coupling in these systems could be obtained from the spectra. The complex AB type splitting patterns and the myriad of small couplings apparent in the saturated proton spectral region were not subjected to simulation attempts.

Conclusions

The ^1H, ^{13}C, and ^{31}P NMR spectra of $[(\eta^5\text{-}C_5H_5)Ru(\eta^4\text{-}COT)(P(OCH_3)_3)]PF_6$, $[(\eta^5\text{-}C_5H_5)Ru(\eta^4\text{-}COD)(P(OCH_3)_3)]PF_6$, $[(\eta^5\text{-}C_5H_5)Ru(\eta^4\text{-}COT)(CO)]PF_6$, and $[(\eta^5\text{-}C_5H_5)Ru(\eta^6\text{-}COT)]PF_6$ have been examined in detail and confirm that the solution and solid state structure of $[(\eta^5\text{-}C_5H_5)Ru(\eta^4\text{-}COT)(P(OCH_3)_3)]PF_6$ are identical. Further investigation of the ^1H NMR spectra of these complexes disclosed the nature of the extensive coupling thoughout the COT ring protons. In addition, ^{31}P decoupled experiments revealed that the phosphorus of the trimethyl phosphite in $[(\eta^5\text{-}C_5H_5)Ru(\eta^4\text{-}COT)(P(OCH_3)_3)]PF_6$ couples to all the cyclooctatetraene ring protons but not to those in the cyclopentadienyl ring.

Acknowledgement

A.M. McNair acknowledges a Louise T. Dosdall Fellowship in Science. This research was supported by Department of Energy grant DOE/DEAC02-83ER13103.

Supplementary Material Available

Listings of thermal parameters, hydrogen atom positional parameters, least-squares planes, dihedral angles, and observed and calculated structure factors has been deposited with NAPS [24].

References

1 T.P. Gill and K.R. Mann, Organometallics, 1 (1982) 485.

2 T.P. Gill, Ph.D. Thesis, University of Minnesota, 1982.

3 A. Efraty, S.S. Sandhu, R. Bystrek and D.Z. Denney, Inorg. Chem., 16 (1977) 2522 and references therein.

4 V.W. Day, I. Tavanaiepour, S.S. Abdel-Meguid, J.F. Kirner, L.-Y. Goh and E.L. Muetterties, Inorg. Chem., 21 (1982) 657 and references therein.

5 D.A. Sweigart, J. Chem. Soc., Chem. Commun., (1980) 1159.

6 R.A. Zelonka and M.C. Baird, J. Organomet. Chem., 228 (1982) 171.

7 All calculations were carried out on PDP 8A and 11/34 computers using the Enraf–Nonius CAD 4-SDP programs. This crystallographic computing package is described in: B.A. Frenz, in H. Schenk, R. Olthof-Hazekamp, H. van Koningsveld, G.C. Bassi (Eds.), Computing in Crystallography, Delft University Press, Delft, The Netherlands, 1978, pp. 64–71. CAD 4SDP Users Manual; Enraf–Nonius: Delft, The Netherlands, 1978.

8 The intensity data were processed as described in: CAD 4 and SDP Users Manual, Enraf–Nonius, Delft, Holland, 1978. The net intensity I is given as: $I = (K/NPI)(C - 2B)$; where $K = 20.1166$ (attenuator factor), NPI = ratio of fastest possible scan rate to scan rate for the measurement, C = total count, and B = total background count. The standard deviation in the net intensity is given by: $\sigma^2(I) = (K/NPI)[C + 4B + pI)^2]$; where p is a factor used to downweight intense reflections. The observed structure factor amplitude F_o is given by; $F_o = (I/Lp)^{1/2}$; where Lp = Lorentz and polarization factors. The $\sigma(I)$'s were converted to the estimated errors in the relative structure factors $\sigma(F_o)$: $(F_o) = [1\sigma(I)/2I]F_o$

9 The function minimized was $\omega(|F_o| - |F_c|)^2$, where $\omega = 1/\sigma^2(F_o)$. The unweighted and weighted residuals are defined as: $R_1 = (\Sigma||F_o| - |F_c||)/\Sigma|F_o|$; $R_2 = [(\Sigma\omega(|F_o| - |F_c|))^2/(\Sigma|F_o|^2)]^{1/2}$. The error in an observation of unit weight is: $[(\Sigma\omega(|F_o| - |F_c|)^2/(NO - NV)]^{1/2}$; where NO and NV are the number of observations and variables, respectively.

10 D.T. Cromer and J.T. Waber, International Tables for X-ray Crystallography, Kynoch Press, Birmingham, England, 1974; Vol. IV, Table 2.2.4. D.T. Cromer, ibid., Table 2.3.1.

11 D.T. Cromer and J.A. Ibers, International Tables for X-ray Crystallography, Kynoch Press, Birmingham, England, 1974; Vol. IV.

12 J.P. Selegue, Organometallics, 1 (1982) 217.

13 G.J. Kruger, A.L. du Preez and R.J. Haines, J. Chem. Soc., Dalton Trans., (1974) 1302.

14 M.I. Bruce, R.C.F. Gardner, J.A.K. Howard, F.G.A. Stone, M. Welling and P.J. Woodward, J. Chem. Soc., Dalton Trans., (1977) 621.

15 H. Schmid and M.L. Ziegler, Chem. Ber., 109 (1976) 132.

16 J. Chatt and L.A. Duncanson, J. Chem. Soc., (1953) 2939.

17 M.A. Bennett, G.B. Robertson and A.K. Smith, J. Organomet. Chem., 43 (1972) C41.

18 B.E. Mann, Adv. Organomet. Chem., 12 (1974) 135.

19 P.W. Jolly and R. Mynott, Adv. Organomet. Chem., 19 (1981) 257.

20 A.N. Nesmeyanov, E.I. Fedin, L.A. Fedorov, P.V. Petrovski, Zh. Strukt. Khim., 13 (1972) 1033.

21 J.G. Verkade, Coord. Chem. Rev., 9 (1972/1973) 1.

22 The magnitude of vicinal coupling constants depend on (1) the dihedral angle ϕ; (2) the bond distance, in this case the Ru–C distances; (3) the valence angles θ and θ' and (4) the electronegativity of the substituents on the atoms in question. Items (2) and (4) are identical for the two sets of protons attached to bound carbons (H(1), H(6) and H(2), H(5)). The differences in coupling must result from differences in either the dihedral or valence angles involved. The dependence of ^3J on the dihedral angle, ϕ is expressed as:

$$^3J = A + B\cos(\theta) + C\cos(2\theta)$$

For organic compounds the constants have the following values: $A \cdot 4.22$, $B\ -0.5$, C 4.5 Hz. While these values would certainly not be valid for the P–H coupling in the system in question, the equation might be expected to give a rough estimate. The dihedral angles P–Ru–C(1)–H(1) and P–Ru–C(6)–H(6) are 48° while the dihedral angles P–Ru–C(2)–H(2) and P–Ru–C(5)–H(5) are 112°. The equation predicts a value of 3/1 for the $^3J_{1,6\text{-P}}/^3P_{2,5\text{-P}}$ ratio, consist with experiment. Empirically, the decrease in the valence angles generally leads to an increase in ^3J coupling, in agreement with the experimental trend.

23 Most ^4J(P–H) couplings that have been measured for organometallic complexes are either zero or very small. For some examples see: (a) M.F. Semmelhack, W. Seufert and L. Keller, J. Organomet. Chem., 226 (1982) 183; (b) D. Catheline and D. Astruc, Organometallics, 3 (1984) 1094; (c) S.J. Young, M.M. Olmstead, M.J. Knudsen and N.E. Schore, Organometallics, 4 (1985) 1432; (d) N.C. Schroeder, J.W. Richardson, Jr., S.-L. Wang, R.A. Jacobson and R.J. Angelici, Organometallics, 4 (1985) 1226.

24 See NAPS document no. 04479 for 14 pages of supplementary material. Order from NAPS c/o Microfiche Publications, P.O. Box 3513, Grand Central Station, New York, N.Y. 101063. Remit in advance in U.S. funds only \$7.75 for photocopies or \$4.00 for microfiche. Outside the U.S. and Canada, add postage of \$4.50 for the first 20 pages and \$1.00 for each of 10 pages of material thereafter, \$1.50 for microfiche postage.